

## ***Supporting Information***

# **Combined experimental and theoretical studies on selective sensing of zinc and pyrophosphate ions by rational designing of compartmental chemosensor probe: Dual sensing behaviour via secondary recognition approach and cell imaging studies**

***Kiran Mawai,<sup>a</sup> Sandip Nathani,<sup>b</sup> Partha Roy,<sup>b</sup> U.P. Singh,<sup>a</sup> Kaushik Ghosh<sup>\*a</sup>***

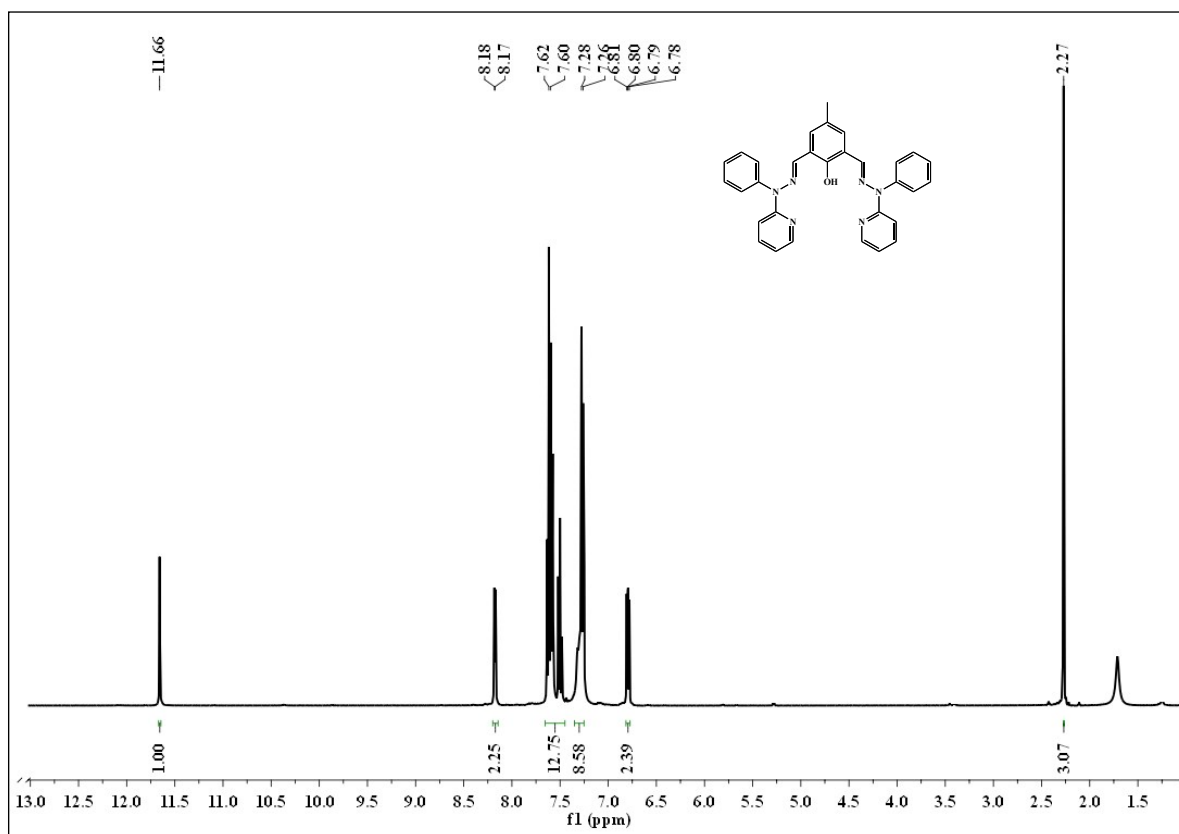
<sup>[a]</sup> *Department of Chemistry, Indian Institute of Technology Roorkee, Roorkee-247667, India*

<sup>[b]</sup> *Department of Biotechnology, Indian Institute of Technology Roorkee, Roorkee-247667, India*

**[ghoshfcy@gmail.com](mailto:ghoshfcy@gmail.com)**

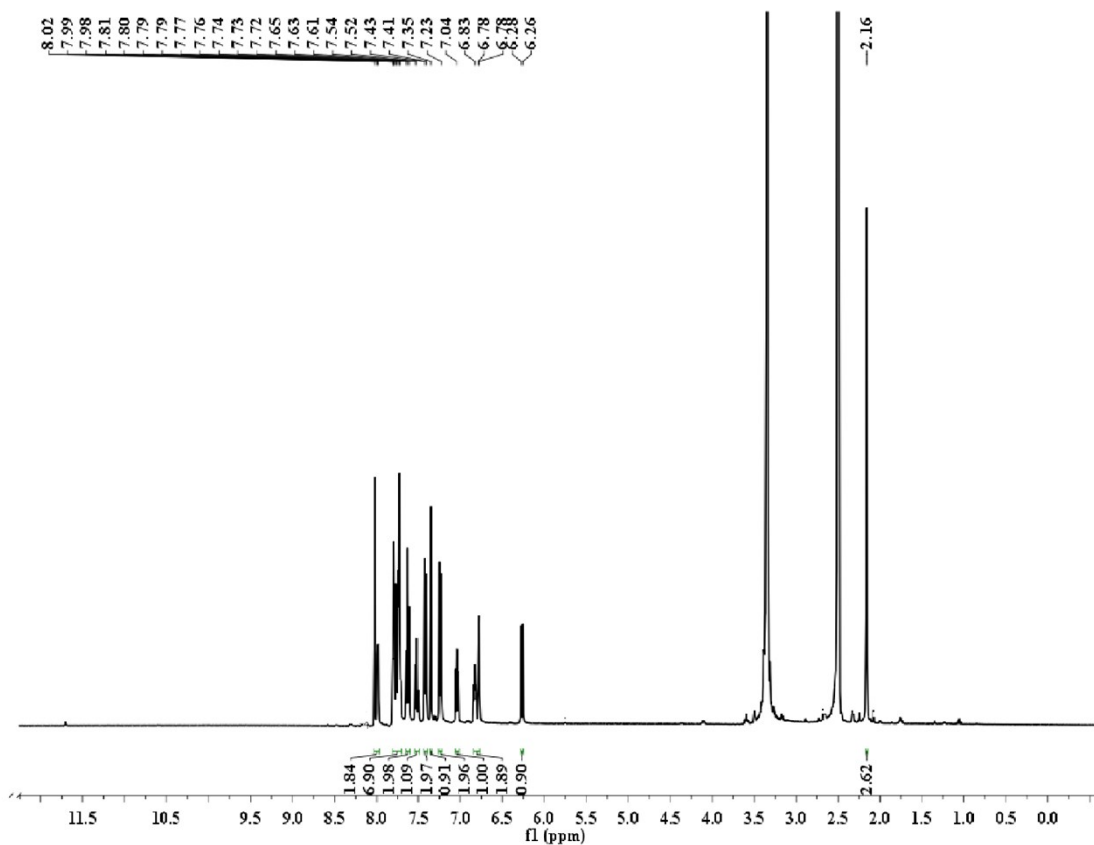
S.No.	Content	Page No.
1	<sup>1</sup> H NMR spectrum of chemosensor HL.....	3
2	<sup>1</sup> H NMR spectrum of zinc complex 2.....	4
3	IR spectra.....	5
4	UV-Vis Spectra of probe HL and zinc complex 2.....	6
5	Detection Limit for Zn <sup>2+</sup> ion and PPI.....	7
6	Sensing study at different pH.....	8
7	Calculation of association constants by fluorescence studies.....	9, 10
8	Job's Plot.....	10
9	Anion binding study of zinc complex 2.....	11
10	HRMS spectrum of HL.....	12
11	HRMS spectrum of HL+Zn <sup>2+</sup> .....	13
12	HRMS spectrum of HL+Zn <sup>2+</sup> +PPI.....	14
13	Cell viability assay.....	15
14	Time resolved measurements.....	16
16	NMR studies.....	17
17	Sensing of different anions by complex 2.....	18
18	Comparison of reported work with present work.....	19
19	References.....	20

## **<sup>1</sup>H NMR spectrum of chemosensor HL**



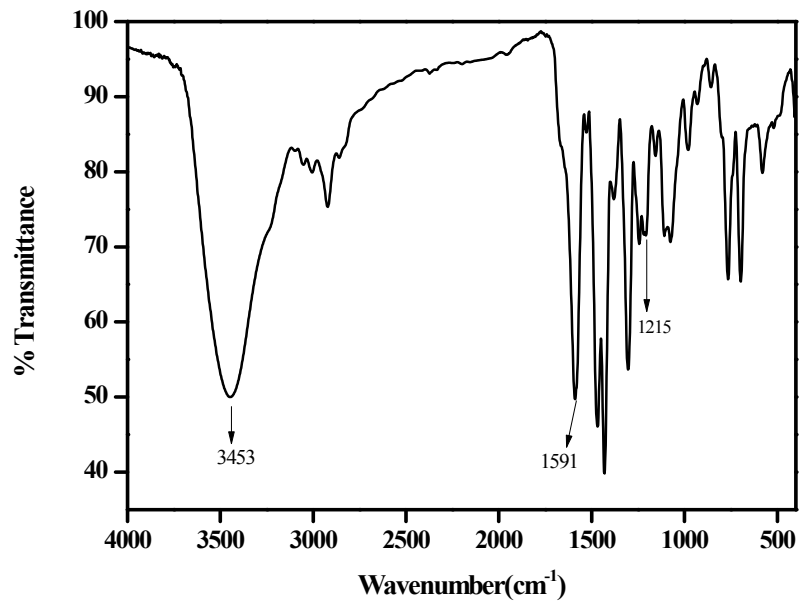
ESI Fig. S1 <sup>1</sup>H NMR spectrum of chemosensor HL.

## **$^1\text{H}$ NMR spectrum of zinc complex 2**

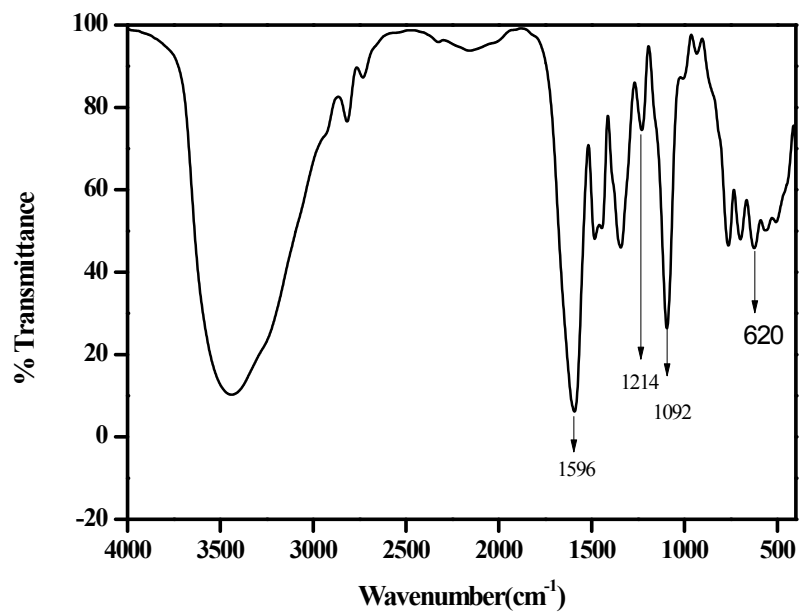


ESI Fig. S2  $^1\text{H}$  NMR spectrum of zinc complex 2.

## IR spectra

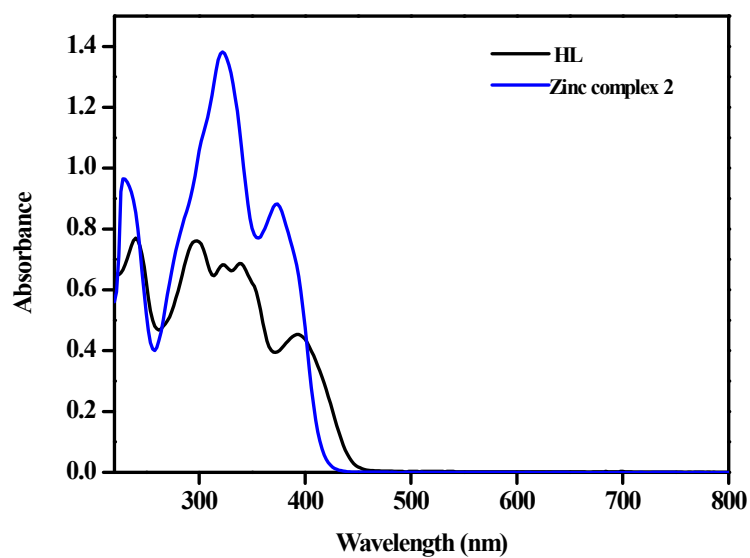


ESI Fig. S3 IR spectrum of probe HL.



ESI Fig. S4 IR spectrum of zinc complex 2.

## UV-Vis Spectra of probe HL and zinc complex 2.



ESI Fig. S5 Absorption spectra of probe HL and zinc complex 2.

Table S1. Molar extinction coefficient values for HL and zinc complex 2.

S.No.	Compounds	Molar extinction coefficient(L mol <sup>-1</sup> cm <sup>-1</sup> )
1	Probe (HL)	$\lambda_{373}$ (15,717), $\lambda_{322}$ (24,633), $\lambda_{238}$ (15,543)
2	Zinc complex 2	$\lambda_{296}$ (48,481), $\lambda_{339}$ (43,670), $\lambda_{393}$ (28,670)

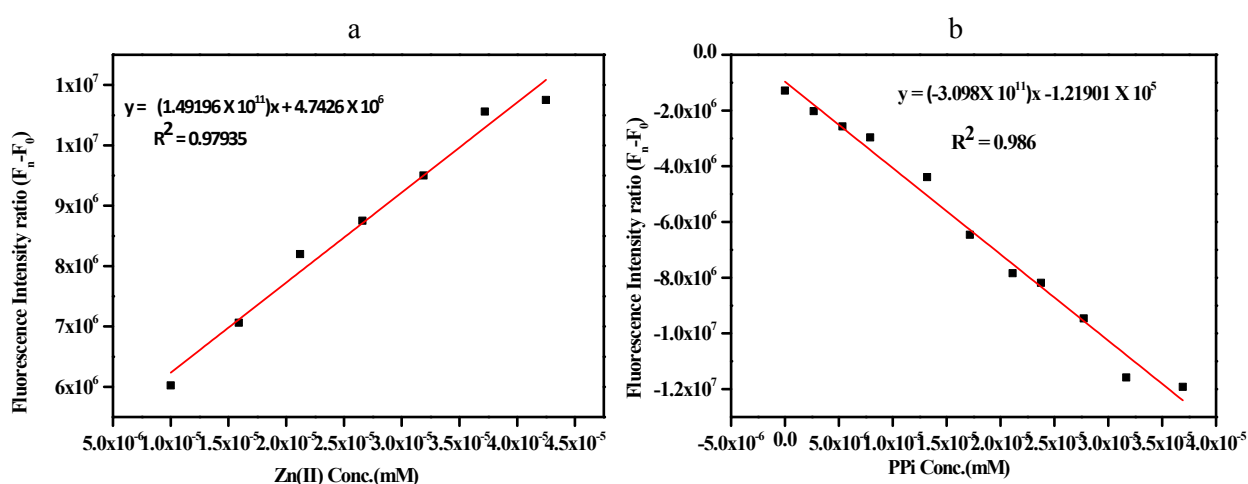
## Detection Limit for Zn<sup>2+</sup> ion and PPI

Based on fluorescence titration, detection limit values for both Zn<sup>2+</sup> and PPI were calculated using the equation  $LOD = 3\sigma/K$ . Where,  $\sigma$  illustrates standard deviation for blank solution of HL. The stock solutions of probe HL, zinc salt and PPI were prepared ( $2 \times 10^{-3}$  M). The fluorescence emission spectrum of HL was measured 10 times, and the standard deviation of blank measurements was achieved. The slope of the fluorescence curve obtained between changes in fluorescence intensities ( $F-F_0$ ) versus Zn<sup>2+</sup> concentration. The  $F$  and  $F_0$  indicate the emission intensities of HL in the presence and absence of Zn<sup>2+</sup> respectively. In similar manner, detection limit for PPI was calculated (Table S2). Where  $F$  and  $F_0$  are the fluorescence intensity of zinc complex (HL+Zn<sup>2+</sup>) in presence and absence of PPI respectively (ESI Fig. S6).

**Detection limit =  $3\sigma/k$**

**Table S2.** LOD values for HL and zinc complex 2

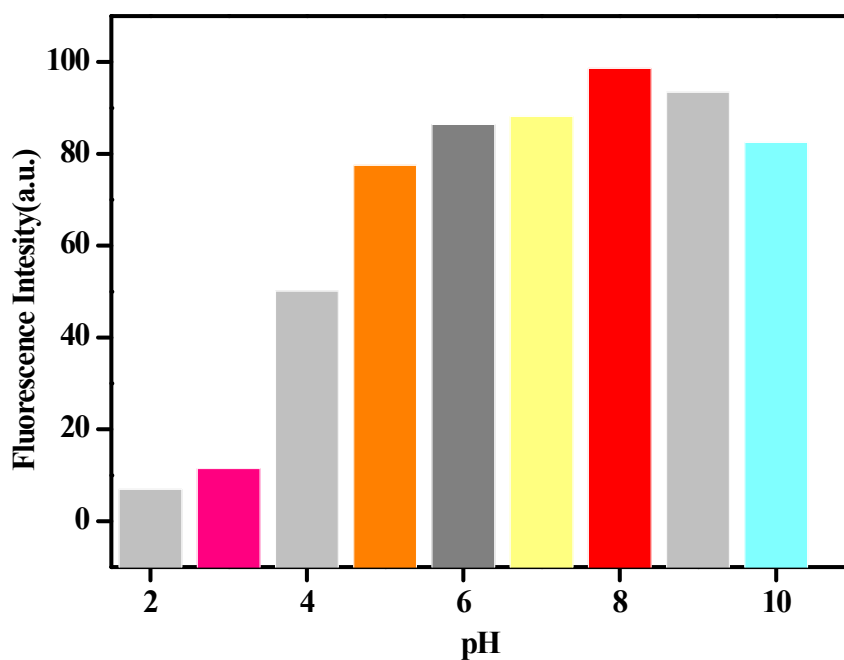
	Standard deviation	Slope	LOD
For Zn <sup>2+</sup>	22715	$1.5184 \times 10^{11}$	$4.48 \times 10^{-7}$
For PPI	55133	$-2.87951 \times 10^{11}$	$5.74 \times 10^{-7}$



**ESI Fig. S6** (a) Calibration curve for HL+Zn<sup>2+</sup> and (b) Calibration curve for PPI (in DMSO: H<sub>2</sub>O (1:9)).

## Sensing study at different pH

To determine the optimum pH conditions for chemosensor HL, fluorometric titration had been carried out by measuring fluorescence intensity at 507 nm. The fluorescence emission intensity of solution of HL and zinc ions (1: 1) at different pH was monitored. Stock solution of HL ( $2 \times 10^{-3}$  M) was prepared in DMSO: H<sub>2</sub>O (1: 9). Different solutions of zinc salt ( $2 \times 10^{-3}$  M) were prepared by using aqueous solution of different pH ranging from 2 to 10. The pH of final solution prepared by mixing HL and zinc salt at particular pH was also maintained accordingly. Then emission intensity at 521 nm was monitored at different pH and was plotted against their respective pH value. Fluorescence intensity was found to be maximum at pH 8 (ESI Fig. S7).



**ESI Fig. S7.** Variation of fluorescence intensity of zinc complex **2** (HL+Zn<sup>2+</sup>) at different pH ranging from 2 to 10.

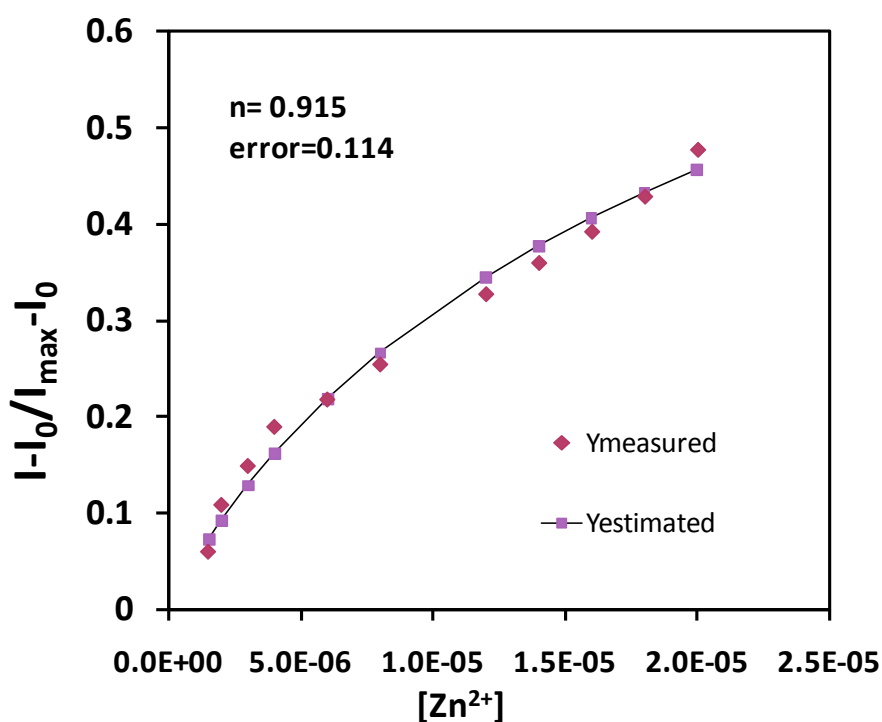


## Calculation of association constants by fluorescence studies

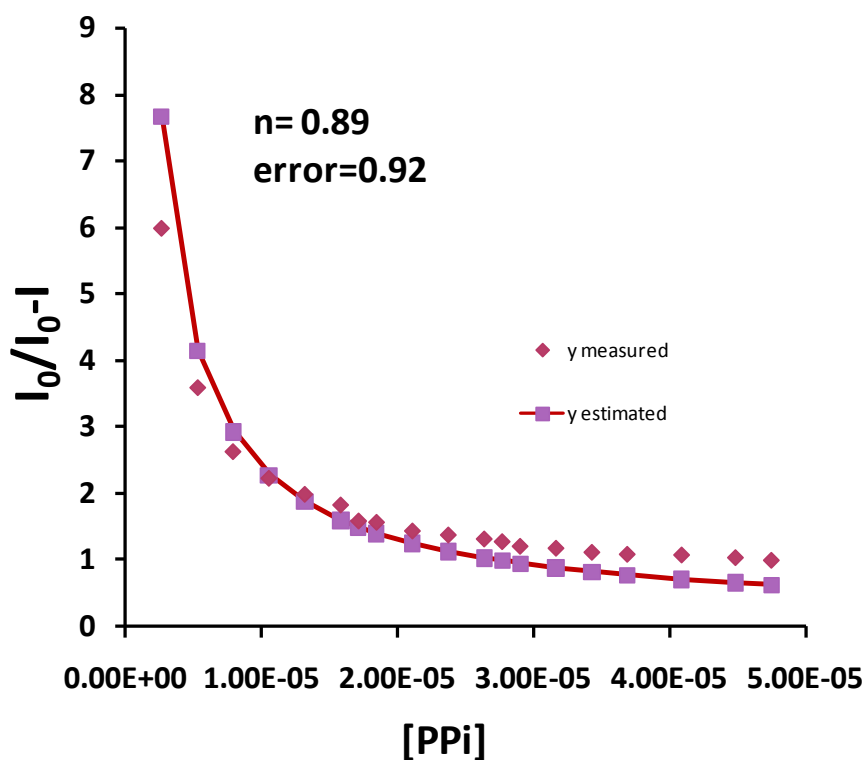
Stock solutions of  $\text{Zn}(\text{ClO}_4)_2$  and chemosensor probe HL having a concentration of  $2 \times 10^{-3}$  M were prepared in DMSO:  $\text{H}_2\text{O}$  (1: 9). The effective  $\text{Zn}^{2+}$  concentration was varied between 0 to  $5 \times 10^{-5}$  M and titrated against  $4 \times 10^{-5}$  M HL.

The binding constant was calculated from nonlinear least square fitting Hill equation<sup>S1</sup>  $[Y = G^n K / (1 + G^n K)]$ , where G is the guest concentration, K is binding constant and n is Hill coefficient. Y was calculated as  $[I - I_0 / I_{\text{max}} - I_0]$ , where  $I_0$ , I and  $I_{\text{max}}$  are the emission intensity at 521 nm in the absence, in the presence and in the presence of an excess amount of  $\text{Cu}^{2+}$ . By plotting Y with respect to  $[\text{Zn}^{2+}]$  the apparent binding constants was obtained as  $1.69 \times 10^4 \text{ M}^{-1}$ .

Similarly the association constant between the  $[\text{HL} + \text{Zn}^{2+}]$  or **2** and PPI ions was analyzed using the fluorescence data with nonlinear least square fitting Hill equation. The association constant for HL with  $\text{Zn}^{2+}$  was calculated to be  $1.69 \times 10^4 \text{ M}^{-1}$  and for zinc complex **2** with PPI was found to be  $4.99 \times 10^5 \text{ M}^{-1}$  using equation<sup>S2</sup>  $y = A + B / (1 + G^n \cdot K_a)$  where Y is  $I_0 / I_0 - I$ , G is the concentration of analyte (PPI) and  $K_a$  is the binding constant (ESI Fig. S8 and S9).



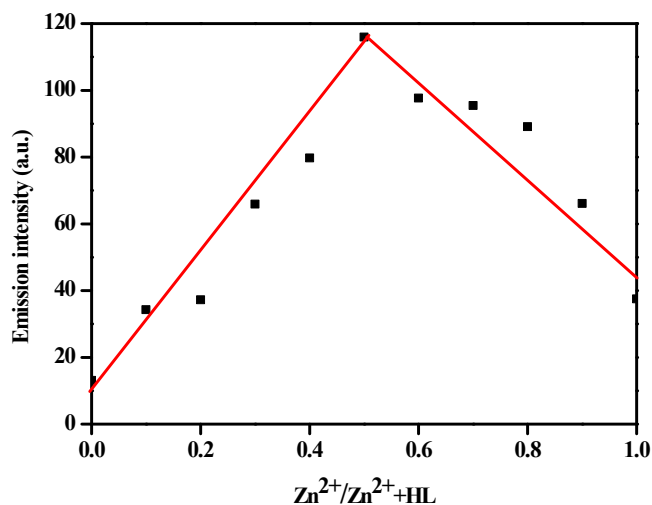
ESI Fig. S8 Non linear Hill plot for the estimation of association constant of zinc ions with probe HL.



ESI Fig. S9 Non linear fit plot for the determination of binding constant for PPI with zinc complex 2 in DMSO: H<sub>2</sub>O (1:9).

### Binding stoichiometry of probe HL and Zn<sup>2+</sup>: Job's Plot

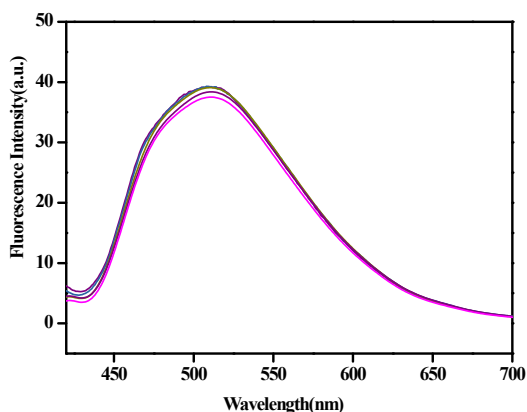
The binding stoichiometry of HL with Zn<sup>2+</sup> was estimated from the Job's plot measurement<sup>S1</sup> on the basis of fluorescence emission intensity. 2 x 10<sup>-3</sup> M stock solution of both HL and Zn<sup>2+</sup> was prepared in DMSO: H<sub>2</sub>O (1:9). Increasing amount of zinc ions were added to fixed amount of HL making final concentration of 0.2 μM. Emission intensity was plotted against mole fraction of Zn<sup>2+</sup>/Zn<sup>2+</sup> + HL at 521 nm. The maxima clearly validated 1: 1 binding stoichiometry of HL with zinc ions (ESI Fig. S10).



**ESI Fig. S10** Job's plot of fluorescence intensity at 521 nm of HL and Zn<sup>2+</sup> ions with a total concentration of 0.2 μM.

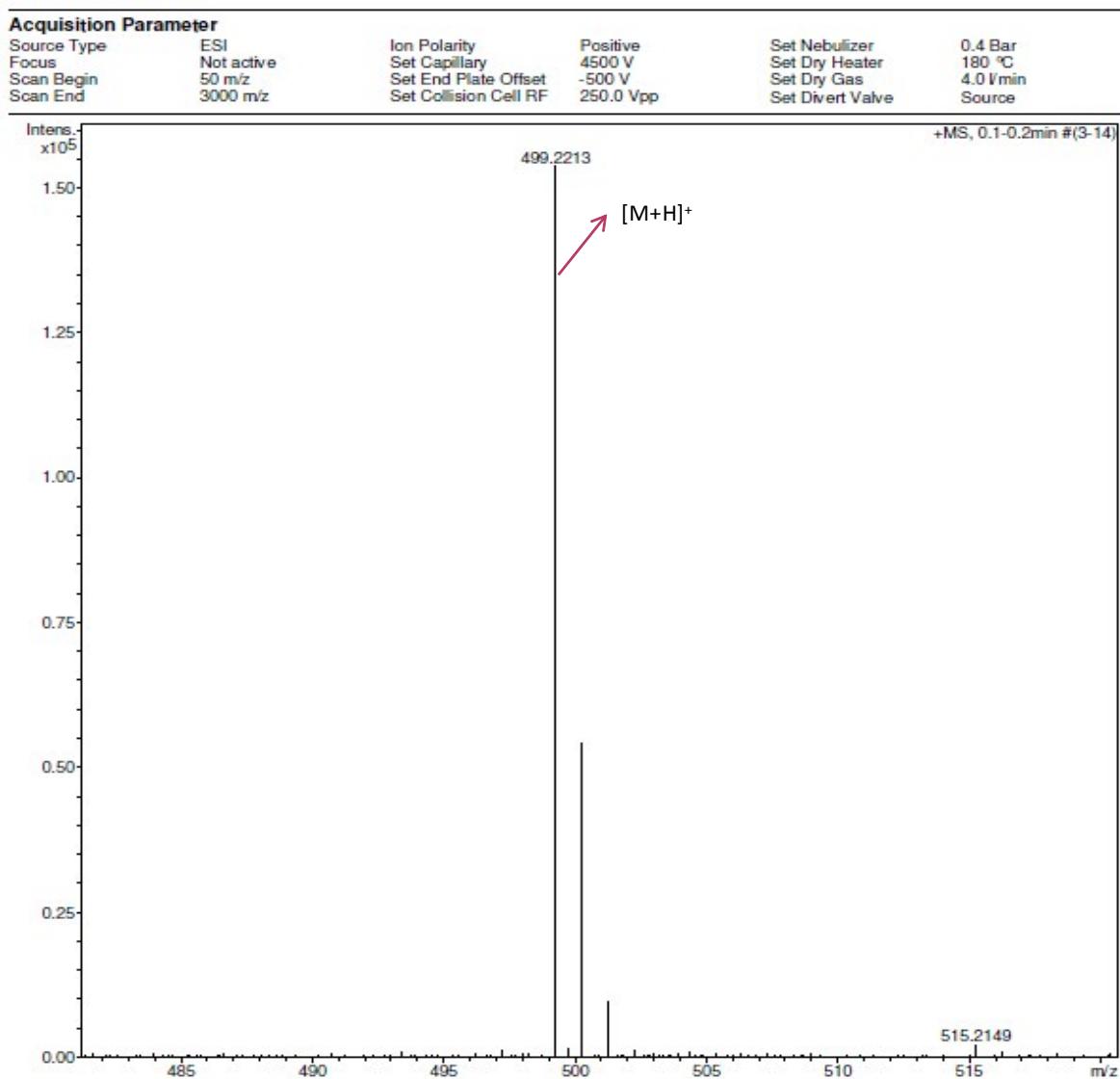
### Anion binding study of zinc complex 2

Addition of ATP also resulted in slight decrement in the emission intensity of complex **2**. To study the effect of ATP on zinc complex **2** further addition of ATP was done with different concentrations. It was observed that fluorescence was quenched only to very small extent and no concentration dependent quenching behaviour was observed on further increasing the concentration of ATP (ESI Fig.S11).



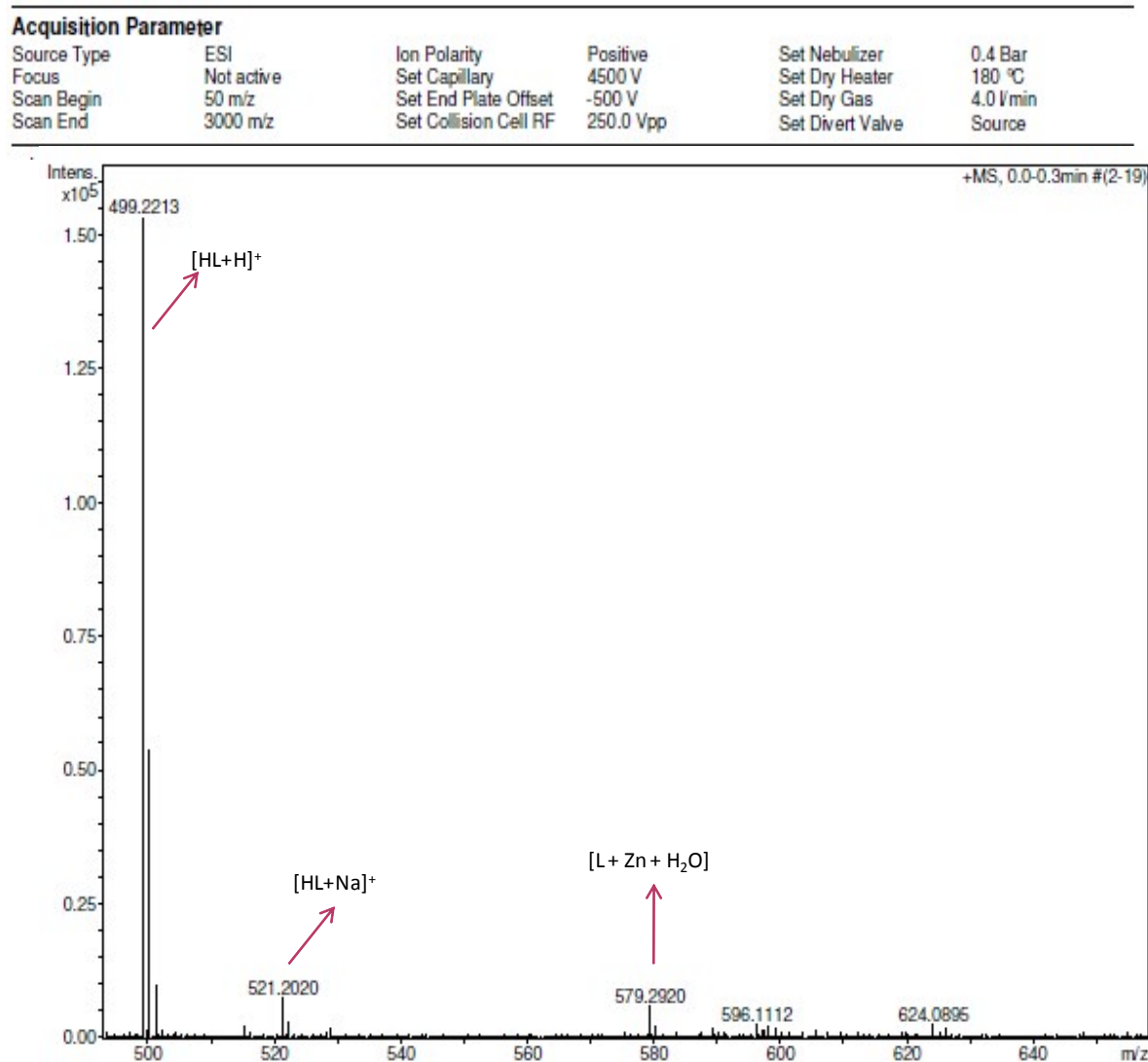
**ESI Fig. S11** Changes in the fluorescence intensity of zinc complex **2** (2 x 10<sup>-5</sup> M) on addition of ATP (2 x 10<sup>-5</sup> M to 8 x 10<sup>-5</sup> M) in DMSO: H<sub>2</sub>O (1:9).

## HRMS spectrum of chemosensor probe HL



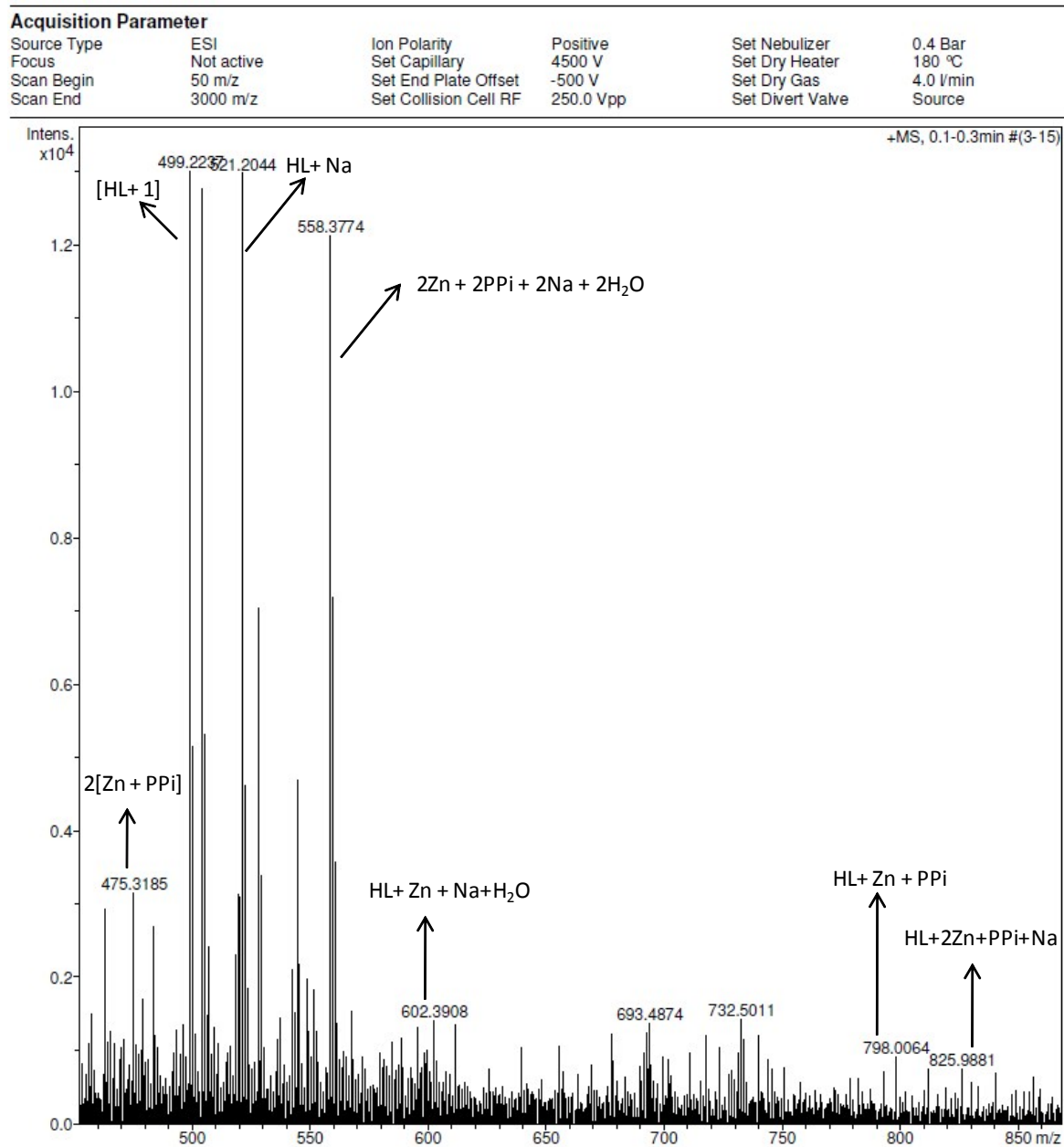
ESI Fig. S12 HRMS spectrum of HL.

## HRMS spectrum of HL +Zn<sup>2+</sup>



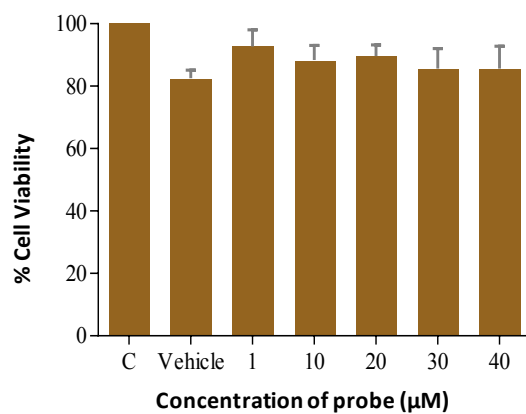
ESI Fig. S13 HRMS spectrum of HL +Zn<sup>2+</sup>.

## HRMS spectrum of zinc complex 2 after addition of PPI.



ESI Fig. S14 HRMS spectrum of 2 + PPI.

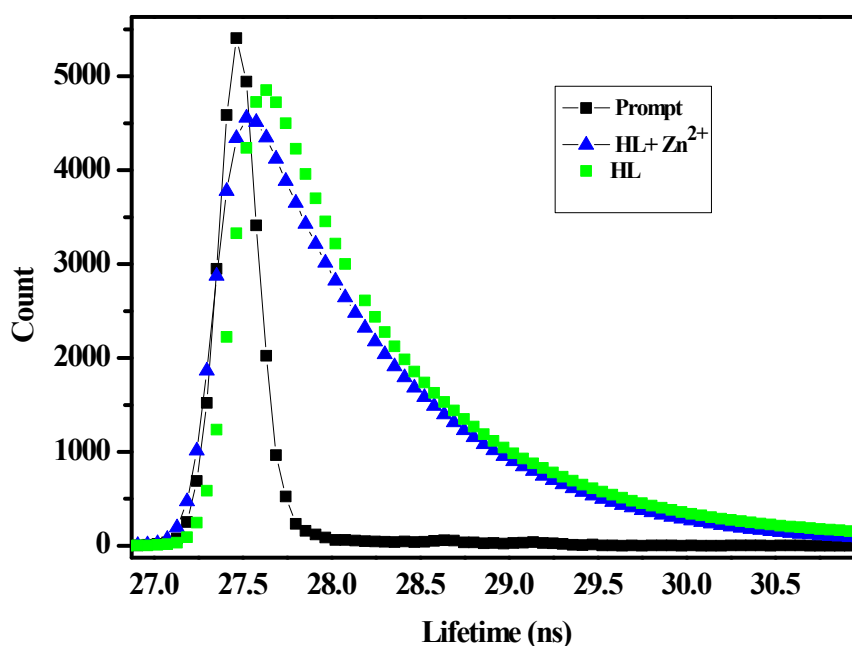
## Cell Viability assay



**ESI Fig. S15** Percentage cell viability of HeLa cells was measured by MTT assay after treatment with different concentrations (1, 10, 20, 30 and 40  $\mu\text{M}$ ) of HL. Results are expressed as the mean of three independent experiments.

## Time resolved measurement

A time-resolved fluorescence technique has been used to examine the excited state behaviour of probe HL and zinc complex in THF solvent. According to the equations<sup>1</sup>  $\tau^{-1} = k_r + k_{nr}$  and  $k_r = \Phi_f/\tau$ . Where  $k_r$  and  $k_{nr}$  are the radiative and nonradiative rate constant respectively.  $\Phi_f$  is the fluorescence quantum yield which was calculated for both probe HL and zinc complex **2**. The fluorescence decay curves of sensor HL and its zinc complex were fitted by biexponential and single exponential functions respectively with acceptable  $\chi^2$  values (ESI Fig. S16).

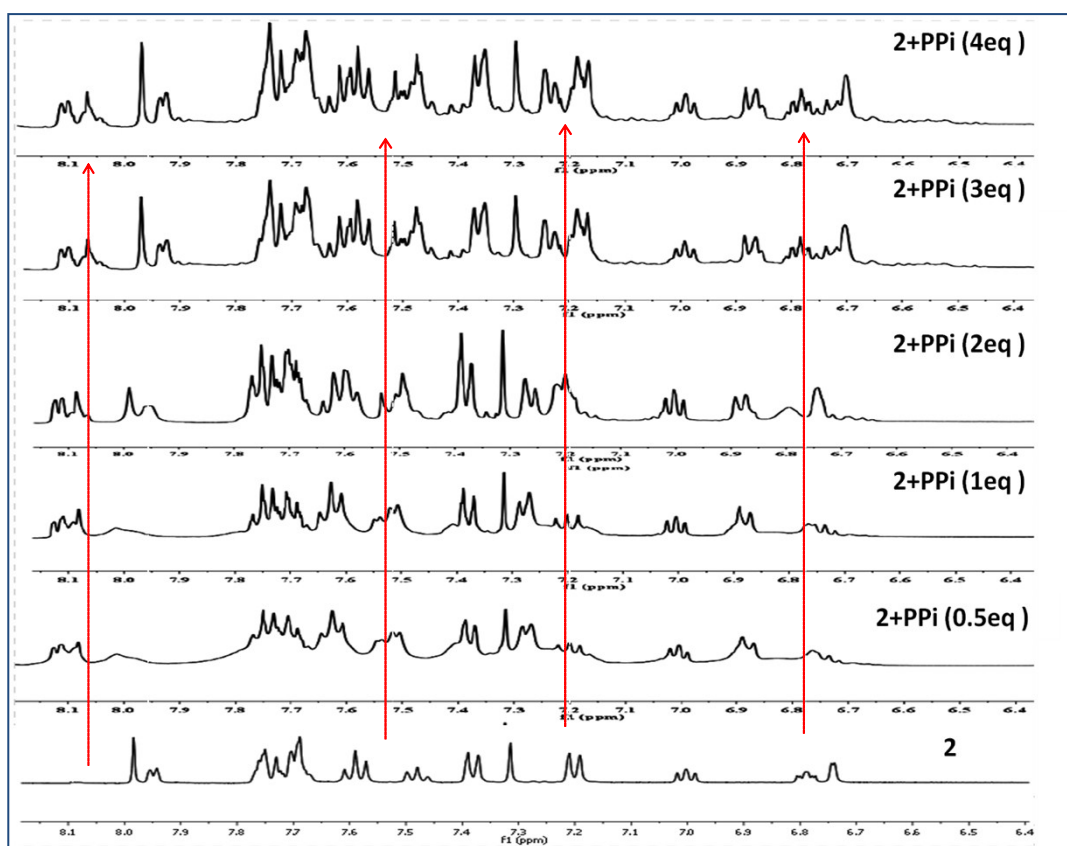


ESI Fig. S16 Time-resolved fluorescence decay of HL (green) and HL+Zn<sup>2+</sup> (blue) ( $\lambda_{ex} = 350$  nm).



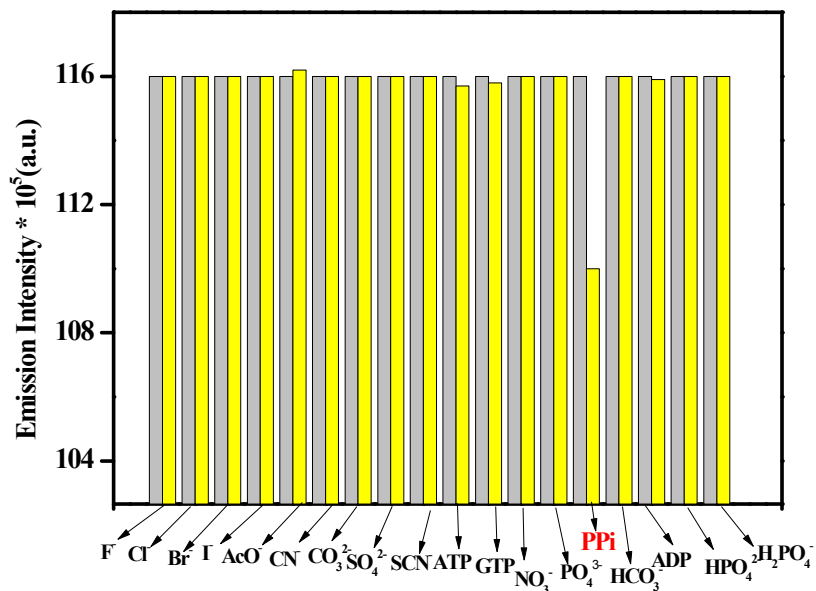
## NMR studies

Proton NMR of complex **2** was carried out in DMSO- $d_6$  while the NMR titration of complex **2** with PPi was performed by taking complex in DMSO- $d_6$  and PPi in  $D_2O$ . The NMR spectra were recorded in JEOL 400 MHz spectrophotometer by applying tetra-methyl-silane (TMS) as an internal standard (ESI Fig. S17).

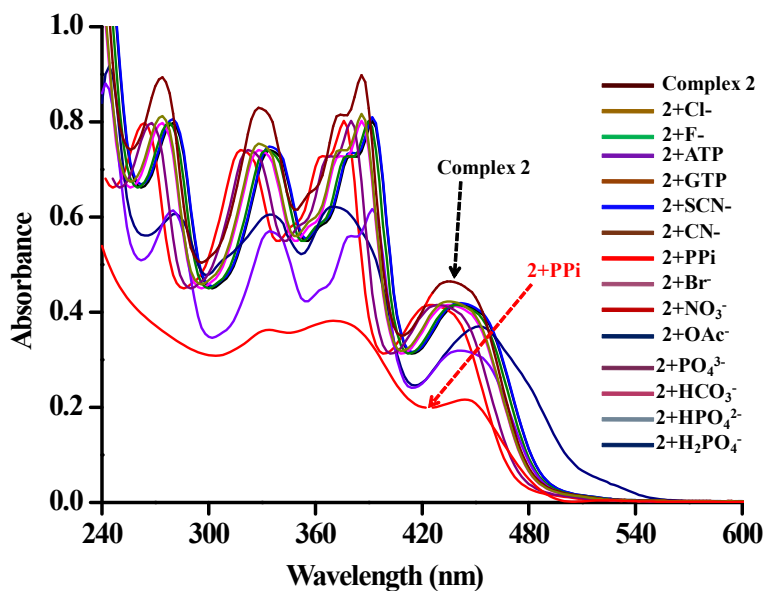


ESI Fig. S17. Changes in  $^1\text{H}$ NMR of complex **2** on subsequent addition of increasing amount of pyrophosphate.complexation of HL with zinc ions.

## Sensing of different anions by complex 2.



ESI Fig. S18. Bar diagram showing the changes in the emission intensity of complex 2 (40 μM) on addition of different anions.



ESI Fig. S19 UV-Vis spectral changes on addition of different anions (40 μM) to zinc complex 2 (40 μM) in DMSO: H<sub>2</sub>O (1: 9).

**Table S3: Comparison of reported work with present work.**

Previous literature	Ligand	Solvent system	Detection limit for zinc	Detection Limit for PPI	Crystal structure	Cell Imaging
Inorg. Chem. 2013, <b>52</b> , 8294. <sup>(53)</sup>	Naphthalene carbohydrazone based	(HEPES) buffer at pH = 7.4	-	155 ppb	No	No
Inorg. Chem. 2013, <b>52</b> , 10052. <sup>(52)</sup>	BODIPY with a hydrazinopyridine unit	Distilled water	-	1.0 $\mu$ M	No	No
New J. Chem., 2016, <b>40</b> , 5976. <sup>(54)</sup>	2,6-diformyl-4-methylphenol and 2-hydrazinyl-4,6-dimethylpyrimidine based	DMSO–H <sub>2</sub> O (1 : 9, 9.727x10 <sup>-7</sup> (M) v/v).	-	-	No	Yes
Inorg. Chem. 2011, <b>50</b> , 1213. <sup>(55)</sup>	DBIQ-based (2,6-bis(5,6-dihydrobenzo[4,5]imidazo[1,2-c]quinazolin-6-yl)-4-methylphenol)	(HEPES) buffer [50 mM, DMSO–H <sub>2</sub> O= 1:9 (v/v), pH = 7.2	3.5 10 <sup>-8</sup> (M)	-	Yes	No
<i>Dalton Trans.</i> , 2014, <b>43</b> , 14701. <sup>(56)</sup>	Anthracene based tripodal tetramine	20% (v/v) water–acetonitrile buffered at pH 7.4 with HEPES	-	0.3 $\mu$ M	No	No
<i>Dalton Trans.</i> , 2014, <b>43</b> , 12689. <sup>(57)</sup>	Pyridine–naphthalene based ligand	CH <sub>3</sub> CN–aqueous HEPES buffer (7/3, v/v, pH = 7.4)	4.6 $\mu$ M	6.3 $\mu$ M	NO	Yes
Inorg. Chem. 2014, <b>53</b> , 6655. <sup>(58)</sup>	Benzoyl hydrazone based	EtOH–H <sub>2</sub> O (1:1)	0.252 nM	7.16 $\times$ 10 <sup>-9</sup> M	Yes	Yes
<i>Anal. Chem.</i> 2013, <b>85</b> , 8369. <sup>(59)</sup>	Quinoline based schiff base	MeOH/aqueous HEPES buffer (1 mM, pH 7.4; 3:2 v/v)	56 ppb	2 ppb	No	No
Present work	2,6-diformyl-4-methylphenol and 2-(1-phenylhydrazinyl)pyridine based	DMSO: H <sub>2</sub> O (1:9 v/v)	4.48 $\times$ 10 <sup>-7</sup> M	5.74 $\times$ 10 <sup>-7</sup> M	Yes	Yes

## References

- (S1) H. P. Fang, M. Shellaiah, A. Singh, M. V. R. Raju, Y. H. Wu, H. C. Lin, *Sens. Actuators B*, 2014, 229.
- (S2) O. G. Tsay, S. T. Manjare, H. Kim, K. M. Lee, Y. S. Lee, D. G. Churchill, *Inorg. Chem.*, 2013, **52**, 10052.
- (S3) S. Anbu, S. Kamalraj, C. Jayabaskaran, and P. S. Mukherjee, *Inorg. Chem.* 2013, **52**, 8294.
- (S4) A. Jana, B. Das, S. K. Mandal, S. Mabhai, A. R. Khuda Bukhshe and S. Dey, *New J. Chem.*, 2016, **40**, 5976.
- (S5) U. C. Saha, B. Chattopadhyay, K. Dhara, S. K. Mandal, S. Sarkar, A. R. Khuda-Bukhshe, M. Mukherjee, M. Helliwell and Pabitra Chattopadhyay, *Inorg. Chem.* 2011, **50**, 1213
- (S6) S. Watchasit, P. Suktanarak, Chomchai Suksai, V. Ruangpornvisuti and T. Tuntulani, *Dalton Trans.*, 2014, **43**, 14701.
- (S7) S. Goswami, A. K. Das, B. Pakhira, S. B. Roy, A. K. Maity, P. Sahab and S. Sarkara, *Dalton Trans.*, 2014, **43**, 12689.
- (S8) S. Anbu, R. Ravishankaran, M. F. C. G. Silva, A. A. Karande, and A. J. L. Pombeiro, *Inorg. Chem.* 2014, **53**, 6655.
- (S9) B. K. Datta, S. Mukherjee, C. Kar, A. Ramesh, and G. Das, *Anal. Chem.* 2013, **85**, 8369.